

Electrochemical Behavior and Sensitive Detection of Luteolin by Graphene-SnO₂ Nanocomposite Modified Electrode

Xiaobao Li¹, Xueliang Niu¹, Wei Chen^{1,2}, Lifeng Dong^{2,3}, Yanyan Niu¹, Taiming Shao⁴, Wenting Lai¹, Wei Sun^{1,*}

¹ Key Laboratory of Tropical Medicinal Plant Chemistry of Ministry of Education, College of Chemistry and Chemical Engineering, Hainan Normal University, Haikou 571158, P R China

² College of Chemistry and Molecular Engineering, Qingdao University of Science and Technology, Qingdao 266042, P R China

³ Hamelin University, Hewitt Avenue, Saint Paul, MN, United States

⁴ Key Laboratory of Medicinal and Edible Plants Resources of Hainan Province, School of Chemical and Material Engineering, Hainan Institute of Science and Technology, Haikou 571126, P R China

*E-mail: swyy26@hotmail.com

Received: 1 June 2017 / Accepted: 17 August 2017 / Published: 12 September 2017

This study utilized a sensitive voltammetric way for detection of luteolin with graphene (GR) and tin oxide (SnO₂) nanocomposite modified electrode. A couple of well-distinctive redox peaks of luteolin could be observed on cyclic voltammogram, which was ascribed to large specific surface area and high conductivity of GR-SnO₂ nanocomposite. Then a new voltammetric sensing method for the analysis of luteolin was established in this experiment. Under the optimized conditions with differential pulse voltammetry, the anodic peak responses enhanced linearly with luteolin concentration from 6.0×10^{-8} mol/L to 6×10^{-5} mol/L with the detection limit of 9.8 nmol/L (3σ). The analytical application of this sensor was successfully proved by the Duiyiwei capsules sample detection.

Keywords: Graphene-SnO₂ nanocomposite, Luteolin, Differential pulse voltammetry, Electroanalysis

1. INTRODUCTION

Luteolin (3',4',5',7'-tetrahydroxyflavone) belongs to flavonoid that is present rich in various plants such as perilla leaf, green pepper, parsley and celery [1], which has lots of pharmacological effects, including anti-inflammatory, anti-allergy, anticancer, anti-oxidation, anti-bacterial and anti-viral [2-4]. Luteolin has also been exhibited to restrain the oxidative injure of biomolecules including DNA, lipid and proteins [5]. Thus it is essential to find a fast, convenient and sensitive procedure to detect luteolin in practical samples. Up to now, a number of techniques have been employed for

luteolin analysis, including HPLC [6-7], GC [8], LC-MS [9-10], fluorimetry [11] and capillary electrophoresis [12-13]. However, some of them are highly priced, time-wasting or with complex experimental procedures. Compared with other methods, electrochemical techniques demonstrate some benefits such as cheap instruments, facility of operation, fast response, high sensitivity and selectivity etc. Also small amounts of samples could be analyzed by microelectrode. For example, Zeng *et al.* fabricated a macroporous carbon modified glassy carbon electrode (GCE) for luteolin detection [14]. Yang *et al.* used a copper nanocluster/graphene (GR) modified electrode for the recognition and analysis of luteolin by differential pulse voltammetry [15]. Ibrahim *et al.* designed In₂O₃ nanoparticles modified GCE for luteolin determination [16]. Wu *et al.* developed a thio- β -cyclodextrin functionalized GR/gold nanoparticles hybrids modified GCE for detection of luteolin [17]. Huang *et al.* used Au-Pd/reduced graphene oxide nanofilm modified GCE for luteolin [18]. Zuo *et al.* applied poly(3,4-ethylenedioxy-thiophene)/manganese dioxide composite modified GCE for electrochemical detection of luteolin [19]. Tang *et al.* fabricated poly(crystal violet)/multi-walled carbon nanotubes modified GCE for electroanalytical determination of luteolin [20]. Abdel-Hamid *et al.* used vulcan carbon black modified GCE for luteolin determination [21]. Our group applied an electrodeposited GR modified electrode as a sensitive platform for detection of luteolin [22].

As an n-type semiconductor with large specific surface area, good biocompatibility and environmental stability, nanosized SnO₂ has been used in electrochemical sensors for a variety of analytes such as folic acid, riboflavin and glucose [23]. SnO₂/GR nanocomposite has been applied in the field of electrochemistry, which exhibits excellent synergistic effects. For example, Baraneedharan *et al.* applied SnO₂/GR nanocomposite modified electrode for the detection of dopamine [24]. Lavanya *et al.* established simultaneous electrochemical determination of epinephrine and uric acid with SnO₂/GR nanocomposite modified electrode [25]. Srivastava *et al.* prepared a NO₂ gas sensor with SnO₂/GR nanocomposite [26]. However, no reports about the application of GR-SnO₂ nanocomposite for the investigation on luteolin electrochemistry had been found.

This paper described a GR-SnO₂ nanocomposite modified electrode with carbon ionic liquid electrode (CILE) as the substrate electrode. Electrochemical investigation on luteolin was researched by GR-SnO₂/CILE with electrochemical parameters calculated. By using GR-SnO₂/CILE as the working electrode, electrochemical method for sensitive analysis of luteolin was established and further used to detection of Duiwei sample with satisfactory results.

2. EXPERIMENTAL

2.1. Materials and apparatus

1-Butylpridinium hexafluorophosphate (BPPF₆, $\geq 99\%$) was purchased from Lanzhou Greenchem. ILS. LICP. CAS. (China) and graphite powder (average particle size 30 μm) was from Shanghai Colloid Chem. Co. (China). GR-SnO₂ nanocomposite was synthesized by a solvothermal method [27]. 1.0×10^{-3} mol/L luteolin (Xi'an Yuquan Biotech. Ltd. Co., China) stocking solution was prepared by anhydrous ethanol. Duiwei soft capsules (Z109700-53) were acquired from Gansu

Duyiwei Pharmaceutical Ltd. Co. (China). All the other reagent were analytical grade and deionized water were used throughout the experiments.

All voltammetric analysis was done on a CHI 1210A electrochemical workstation with electrochemical impedance spectroscopy (EIS) on a CHI 750B electrochemical workstation (Shanghai CH Instrument, China). A conventional three-electrode system was constructed using Pt wire as the counter electrode, saturated calomel electrode (SCE) as the reference electrode and modified CILE ($\Phi=4$ mm) as the working electrode.

2.2. Fabrication of GR-SnO₂/CILE

CILE was prepared with the mixture of BPPF₆ and graphite powder (mass ratio 1:2), which was filled into one end of a glass electrode tube with a copper wire inserted through the opposite end to set up an electrical contact. Then 6.0 μ L of 0.5 mg/mL GR-SnO₂ nanocomposite was casted on CILE surface and dried at room temperature. During this procedure, a glass container was covered on the electrode surface to evaporate the water slowly in air. The prepared GR-SnO₂/CILE was stored at 4°C refrigerator when not in use.

2.3. Electrochemical detection

The luteolin or sample solution was mixed with 0.1 mol/L B-R buffer (pH 4.0). Cyclic voltammetry was scanned in the range from 0 to 1.0 V at the scan rate of 0.1 V/s and differential pulse voltammetry was recorded from 0.1 V to 0.8 V with pulse amplitude as 50 mV, pulse width as 0.2 s and pulse period as 0.5 s.

3. RESULTS AND DISCUSSION

3.1. EIS of the modified electrodes

The impedance changes during the electrode modification can be checked by EIS, which provide the interface resistance and reflect the interfacial conductivity. The electron transfer resistance (Ret) is related to the dielectric and insulating features at the electrode/electrolyte interface. As shown in Fig. 1, the Ret results of CILE and GR-SnO₂/CILE were got as 43.65 Ω and 20.58 Ω , which indicated that GR-SnO₂ nanocomposite exhibited good conductivity with the interfacial resistance decreased. GR has high conductivity with large surface area, which can load other materials and the nanocomposite exhibits the synergistic effects. Therefore the synergistic effects between GR and SnO₂ resulted in the enhancement of interfacial conductivity with the resistances decreased [27].

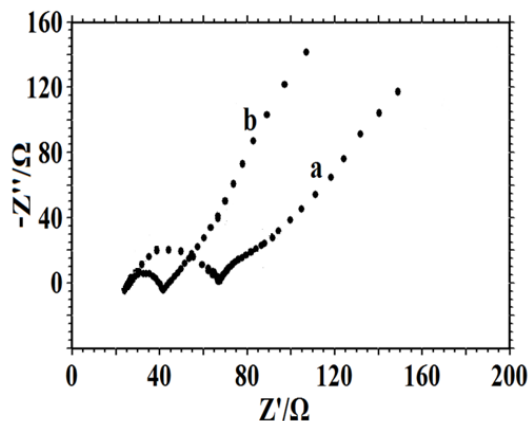


Figure 1. EIS of (a) CILE and (b) GR-SnO₂/CILE in the presence of 10.0 mmol/L [Fe(CN)₆]^{3-/4-} and 0.1 mol/L KCl solution with frequency range from 10⁴ to 0.1 Hz.

3.2. Cyclic voltammetric behaviors of luteolin

Cyclic voltammetric behaviors of 1.0 μmol/L luteolin on different working electrodes were recorded in a 0.1 mol/L B-R (pH 4.0) at a scan rate of 100 mV/s with the curves shown in Fig. 2. On CILE (curve b) the redox peak potentials of luteolin were 0.544 V (*E_{pa}*) and 0.515 V (*E_{pc}*). The values of *I_{pa}* and *I_{pc}* were found to be 1.89 μA and 1.47 μA. While on GR-SnO₂/CILE (curve a), the redox peak potentials of luteolin were 0.552 V (*E_{pa}*) and 0.510 V (*E_{pc}*) with the peak-to-peak separation (ΔE_p) as 42 mV and the redox peak currents of luteolin increased greatly with values of 3.94 μA (*I_{pa}*) and 3.07 μA (*I_{pc}*). The values of redox peak currents were about 2.08 times larger than that of CILE, which could be attributed to the high conductive GR-SnO₂ nanocomposite on the electrode surface. The presence of GR-SnO₂ nanocomposite was beneficial for the fastening of the electron transfer and acted as the electron bridges to improve the electrochemical performance of electrode, which accelerated the electron transfer between luteolin and electrode. Therefore the electrochemical analysis of luteolin was strengthened with better reversibility.

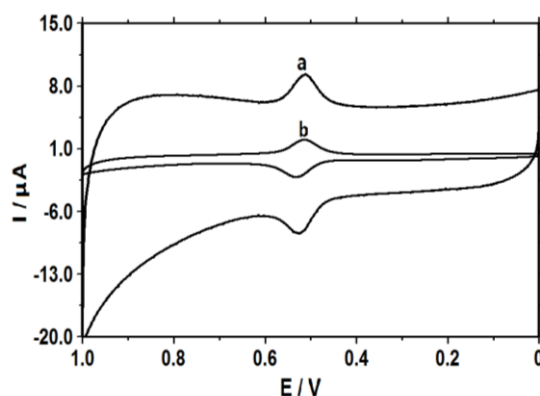


Figure 2. Cyclic voltammograms of 1.0 μmol/L luteolin on (a) GR-SnO₂/CILE and (b) CILE with scan rate as 100 mV/s.

3.3. Electrochemical investigation

The effect of buffer pH on the voltammetric results of 1.0 $\mu\text{mol/L}$ luteolin on GR-SnO₂/CILE was checked in the pH range from 2.0 to 7.0 with the curves shown in Figure 3A. It can be found that a pair of redox peaks appeared at different buffer pH, indicating that protons influenced the electrochemical reaction. The relationship of buffer pH on the oxidation peak current was plotted as Figure 3B, which had the maximum value at pH 4.0. Therefore pH 4.0 was selected as the optimal buffer, which could provide more protons for the electrode reaction. Figure 3C showed that the linear regression relationship of the formal peak potential ($E^{0'}$) with pH and the equation was $E^{0'}(\text{V}) = -0.0662\text{pH} + 0.799$ ($\gamma=0.999$). The slope value (-66.2 mV/pH) was close to the theoretical value (-59 mV/pH), indicating that an equal number of protons and electrons were taken part in the electrochemical reaction.

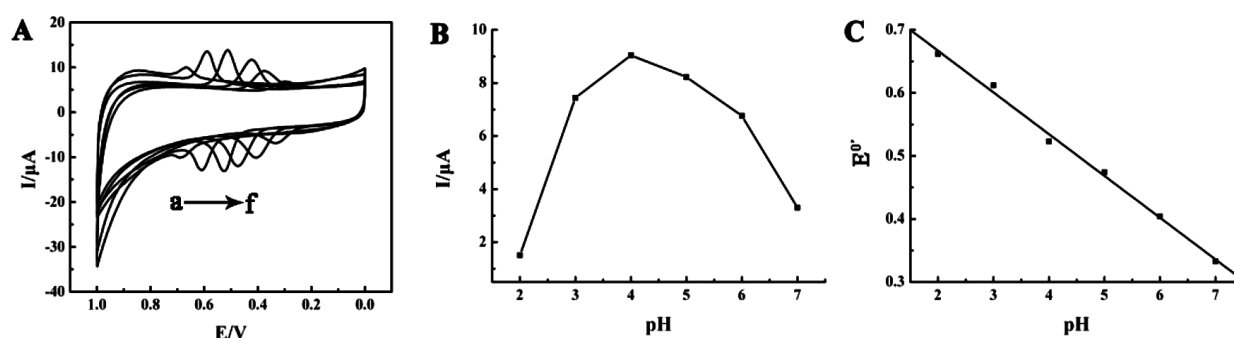


Figure 3. (A) Cyclic voltammograms of 1.0 $\mu\text{mol/L}$ luteolin on GR-SnO₂/CILE with different buffer pH (from a to f: 2.0, 3.0, 4.0, 5.0, 6.0, 7.0) at the scan rate of 100 mV/s; (B) Relationship of I_{pa} against pH; (C) Relationship of the formal peak potential ($E^{0'}$) against pH.

Figure 4A showed the results of scan rate on the electrochemical behavior of 1.0 $\mu\text{mol/L}$ luteolin on GR-SnO₂/CILE by cyclic voltammetry. From 20 mV/s to 500 mV/s the redox peak currents increased gradually with scan rate and the relationship of I_p with v was obtained in Figure 4B with two linear regression equations as I_{pa} (μA) = $-0.0969v + 0.183$ (V/s) ($\gamma=0.999$) and I_{pc} (μA) = $0.0835v - 0.145$ (V/s) ($\gamma=0.999$), indicating an adsorption process. The presence of GR-SnO₂ nanocomposite on the electrode had large surface area for the adsorption of more luteolin on the electrode surface.

Along with the increase of scan rate, the oxidation peak potentials moved positively and the reduction peak potential moved negatively, demonstrating the redox irreversibility of luteolin was increased with a quasi-reversible process [22]. As shown in Figure 4C, the relationship of the peak potentials with $\ln v$ were also calculated with regression equations as E_{pa} (V) = $0.0455 \ln v$ (V/s) + 0.578 ($\gamma=0.992$) and E_{pc} (V) = $-0.0376 \ln v$ (V/s) + 0.464 ($\gamma=0.994$). According to Laviron's equation [28], electrochemical parameters could be calculated with the charge transfer coefficient (α) as 0.54, the apparent heterogeneous electron transfer rate constant (k_s) as 1.9 s^{-1} and the electron transfer number (n) as 1.26. Because the number of proton and electron in the electrode reaction was the same, then one proton was involved in the electrode reaction, with the reaction mechanism expressed as

scheme 1, which involved the oxidation of 4'-hydroxyl on the benzene ring with one electron and one proton on the forward process and reduced at the backward scan [29].

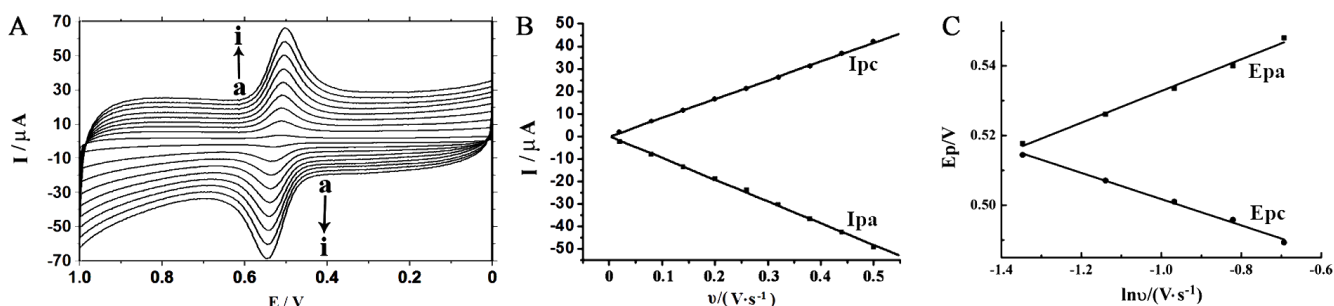
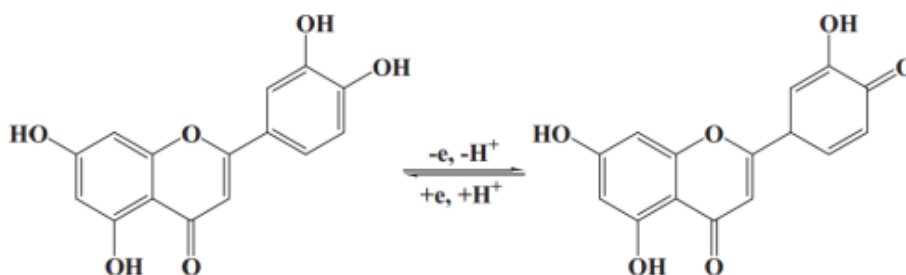


Figure 4. (A) Cyclic voltammograms of 1.0 μmol/L luteolin on GR-SnO₂/CILE in pH 4.0 B-R buffer at various scan rates (from a to i as 40, 60, 80, 100, 150, 200, 300, 400, 500 mV/s); (B) Linear relationship of the redox peak currents versus scan rate (v); (C) Linear relationship of the redox peak potentials versus $\ln v$.



Scheme 1. Electrochemical reaction mechanism of luteolin on the electrode

3.4. Calibration curve

At the optimal conditions luteolin standard solutions at different concentration were measured by differential pulse voltammetry (DPV) with the typical voltammograms shown in Figure. 5A and the calibration curves shown in Figure 5B and 5C. The oxidation peak currents increased with luteolin concentration from 0.06 μmol/L to 2.0 μmol/L and 4.0 μmol/L to 60.0 μmol/L with the linear regression equation as $I_{pa} (\mu A) = 0.33 C (\mu mol/L) + 1.60$ ($\gamma=0.995$) and $I_{pa} (\mu A) = 1.52 C (\mu mol/L) - 0.12$ ($\gamma=0.995$). The detection limit of luteolin with GR-SnO₂/CILE was estimated to be 0.0098 μmol/L ($3S_0/S$), where 3 is the factor at the 99% confidential level, S_0 is the standard deviation of the blank measurements without luteolin ($n=9$) and S is the slope value of the calibration curve.

Also the linear range and detection limit for the electrochemical analysis of luteolin by different working electrodes were summarized in table 1. It can be seen that on GR-SnO₂/CILE a wider detection range and lower detection limit could be achieved with good sensitivity, which proved the successful fabrication of a new voltammetric method for luteolin detection.

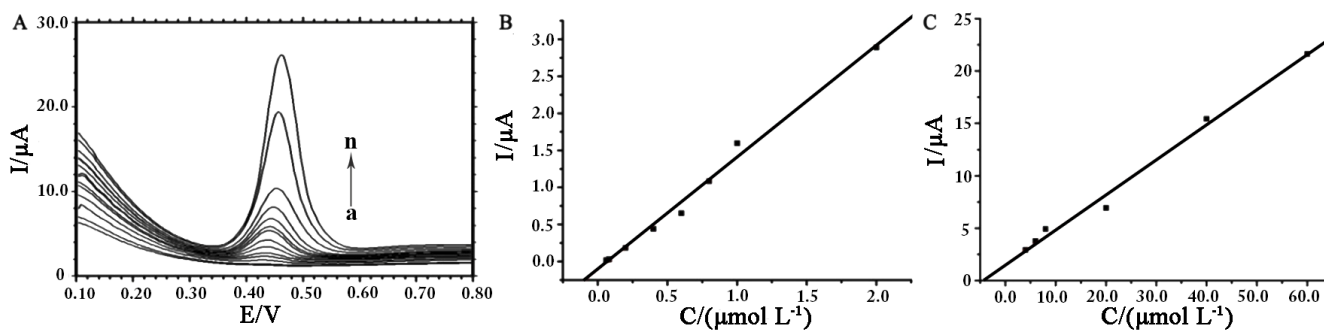


Figure 5 (A) DPV curves of different luteolin concentrations on GR-SnO₂/CILE in 0.1 mol/L pH 4.0 B-R buffer (from a to n: 0.06, 0.08, 0.2, 0.4, 0.6, 0.8, 1.0, 2.0, 4.0, 6.0, 8.0, 20.0, 40.0, 60.0 μmol/L); Calibration curves for (B) 0.06~2.0 μmol/L and (C) 4.0~60.0 μmol/L luteolin.

Table 1. Comparison of the analytical parameters for electroanalysis of luteolin.

Electrode	Linear range (mol/L)	Detection limit (mol/L)	Reference
MPC/GCE	$3.0 \times 10^{-7} - 3.0 \times 10^{-5}$	1.3×10^{-9}	14
Au-Pd/rGO/GCE	$1.0 \times 10^{-8} - 8.0 \times 10^{-5}$	9.8×10^{-10}	18
PEDOT/MnO ₂ /GCE	$5.0 \times 10^{-9} - 7.0 \times 10^{-6}$	1.8×10^{-9}	19
PCV/MWCNTs/GCE	$2.0 \times 10^{-8} - 7.0 \times 10^{-5}$	5.0×10^{-9}	20
VCB/GCE	$2.4 \times 10^{-9} - 5.14 \times 10^{-8}$	2.21×10^{-9}	21
GNs/HA/GCE	$2.0 \times 10^{-8} - 1.0 \times 10^{-5}$	1.0×10^{-8}	30
GCE	$1.0 \times 10^{-8} - 1.0 \times 10^{-6}$	5.0×10^{-9}	31
HPLDE	$4.0 \times 10^{-9} - 1.0 \times 10^{-6}$	1.0×10^{-9}	32
Au-BMIPF ₆ -CPE	$1.0 \times 10^{-7} - 5.8 \times 10^{-6}$	2.8×10^{-8}	33
CS-GR/GCE	$2.0 \times 10^{-9} - 6.0 \times 10^{-5}$	5.93×10^{-10}	34
Au/3DGR/CILE	$5.0 \times 10^{-8} - 5.0 \times 10^{-5}$	7.59×10^{-9}	35
PDDA-G-CNTs/ β -CD/GCE	$5.0 \times 10^{-8} - 6.0 \times 10^{-5}$	2.0×10^{-8}	36
Ag-BMIPF ₆ biosensor	$9.9 \times 10^{-8} - 5.8 \times 10^{-6}$	5.4×10^{-8}	37
HA-CNT	$4.0 \times 10^{-7} - 1.2 \times 10^{-5}$	8.0×10^{-7}	38
GR-SnO ₂ /CILE	$6.0 \times 10^{-8} - 6.0 \times 10^{-5}$	9.8×10^{-9}	this work

MPC: Macroporous carbon, GCE: Glassy carbon electrode, rGO: Reduced graphene oxide, PEDOT: Poly(3,4-ethylenedioxythiophene), PCV: Poly(crystal violet), VCB: Vulcan carbon black, GNs: Graphene nanosheets, HA: Hydroxyapatite, HPLDE: Heated pencil lead disk electrode, BMIPF₆: 1-Butyl-3-methylimidazolium hexafluorophosphate, CPE: Carbon paste electrode, CS: Chitosan, MWCNT: Multi-walled carbon nanotubes, PDDA-G-CNTs: Poly(diallyldimethylammonium chloride)-graphene-carbon nanotubes hybrid, β -CD: β -cyclodextrin.

3.5. Interference

The influences of coexisting compounds on the analysis of 1.0 μmol/L luteolin were checked and the data were listed in table 2. By the addition of these compounds in luteolin standard solution,

the voltammetric responses were recorded and the changes before and after the addition were calculated. As shown in table 2 few of them influenced the analytical results with the relative errors less than $\pm 5\%$, indicating the good selectivity for luteolin analysis. The results could be due to the fact that the potential co-existing substances had no obvious electrochemical response at the oxidation potential for luteolin determination.

3.6. Reproducibility and stability

Reproducibility of the detection by GR-SnO₂/CILE was evaluated by four times detections of a luteolin solution (1.0 $\mu\text{mol/L}$) with the relative standard deviation (RSD) as 3.0%. Stability of GR-SnO₂/CILE was checked by 40 cyclic scanning in pH 4.0 B-R and the background responses kept almost unchanged. Also the long-term stability of GR-SnO₂/CILE was tested by storing the electrode at room temperature for 10 days and the oxidation current of luteolin was about 90% of its initial data. These results demonstrated that GR-SnO₂/CILE had excellent stability and reproducibility. Therefore GR-SnO₂/CILE could be used as a reliable method for the determination of luteolin.

Table 2. Influence of coexisting compounds on the detection of 1.0 $\mu\text{mol/L}$ luteolin (n=3)

Coexisting Substances	Concentration ($\mu\text{mol/L}$)	Relative error (%)	Coexisting substances	Concentration ($\mu\text{mol/L}$)	Relative error (%)
L-Threonine	100.0	2.42	L-Proline	100.0	0.90
L-Arginine	100.0	2.07	Cd ²⁺	100.0	1.27
L-Cystine	100.0	3.34	Ba ²⁺	100.0	3.32
L-Alanine	100.0	1.29	Co ²⁺	100.0	3.17
L-Leucine	100.0	1.73	K ⁺	100.0	4.15
L-Tryptophane	100.0	1.39	Na ⁺	100.0	4.21
L-Lysine	100.0	3.57	Mn ²⁺	100.0	2.12

3.7. Analytical application

The luteolin content in Duyiwei soft capsules was determined by GR-SnO₂/CILE with the following procedure. Five capsules were finely pulverized with the powder dissolved with ethanol. Then the mixture was sonication for 30 min and refluxed for 120 mins, the turbid liquid was filtered carefully and the clear filtrate was diluted by pH 4.0 B-R buffer solution to get the sample solution, which was detected by the experiment method with the content shown in table 3. The recovery test was checked by the addition of the standard luteolin solution in the sample solution, which was in the range from 97.55% to 104.11 % with the RSD less than 4.0 %. The results indicated that the proposed method with GR-SnO₂/CILE as the working electrode could be used for luteolin analysis in real samples with satisfactory results.

Table 3. Determination of luteolin concentration in Duiyiwei capsules (n=3)

Samples	Detected ($\mu\text{mol/L}$)	Added ($\mu\text{mol/L}$)	Total ($\mu\text{mol/L}$)	Recovery (%)	RSD (%)
1	0.130	0.1	0.250	104.11	3.74
2	0.120	0.1	0.210	97.55	2.12
3	0.170	0.1	0.260	103.42	2.55

4. CONCLUSION

In this paper a GR-SnO₂ nanocomposite was modified on CILE to get GR-SnO₂/CILE, which exhibited excellent electrochemical performance due to its specific properties. Electrochemistry of luteolin was realized and enhanced on GR-SnO₂/CILE with electrochemical kinetic parameters calculated. This fabricated electrode was further used for the analysis of luteolin content in Duiyiwei soft capsules with the satisfactory results. All the results proved that GR-SnO₂/CILE nanocomposite modified electrode could be used in the drug analysis with the advantages including faster response, wider linear and lower detection limit, good stability and reproducibility.

ACKNOWLEDGEMENTS

This project was financially supported by the Program for Innovative Research Team in University (IRT-16R19), the National Natural Science Foundation of China (21362009, 81360478), the Natural Science Foundation of Hainan Province (2017CXTD007, 20162031), the Research Project of Hainan Provincial Department of Education (Hnky2017-21) and the Graduate Student Innovation Research Project of Hainan Province (Hyb2017-35).

References

1. C. W. I. Haminiuk, G. M. P. Maciel, M. S. V. P. Oviedo and R. M. Peralta, *Food Sci. Technol.*, 47 (2012) 2023.
2. Y. Lin, R. Shi, X. Wang and H.M. Shen, *Curr. Cancer Drug Tar.*, 7 (2008) 634.
3. H. Kikuzaki, M. Hisamoto, K. Hirose, K. Akiyama and H. Taniguchi, *J. Agr. Food Chem.*, 50 (2002) 2161.
4. D. M. Zhao, X. H. Zhang, L. J. Feng, Q. Qi and S. F. Wang, *Food Chem.*, 127 (2011) 694.
5. K. Kazuki, U. Mari, Y. Hiroaki and H. Takashi, *Arch. Biochem. Biophys.*, 455 (2006) 197.
6. F. M. Areias, P. Valentao, P. B. Andrade, F. Ferreres and R. M. Seabra, *Food Chem.*, 73 (2001) 307.
7. S. M. Wittemer and M. J. Veit, *J. Chromatogr. B*, 793 (2003) 367.
8. C. S. Liu, Y. S. Song, K. J. Zhang, J. C. Ryu, M. Kim and T. H. Zhou, *J. Pharm. Biomed. Anal.*, 13 (1995) 9.
9. J. G. Renee, C. K. Geoffrey, A. Z. Mamdouh and J. A. Louise, *Phytochem. Anal.*, 11 (2000) 257.
10. D. A. Van Elswijk, U. P. Schobel, E. P. Lansky and H. Irth, J. van der Greef, *Phytochem.*, 65 (2004) 233.
11. G. Favaro, C. Clementi, A. Romani and V. Vickackaite, *J. Fluoresc.*, 17 (2007) 707.
12. X. Xu, L. Yu and G. Chen, *J. Pharm. Biomed. Anal.*, 41 (2006) 493.
13. Y. Cao, Q. Chu, Y. Fang and J. Ye, *Anal. Bioanal. Chem.*, 374 (2002) 294.

14. L. J. Zeng , Y. F. Zhang , H. Wang and L.P. Guo, *Anal. Methods*, 5 (2013) 3365.
15. T. J. Yang and D. Jiang, *Asian J. Chem.*, 25 (2013) 8388.
16. H. Ibrahim and Y. Temerk, *Sensor. Actuat. B-Chem.*, 206 (2015) 744.
17. T. X. Wu, Z. G. Liu, Y. J. Guo and C. Dong, *J. Electroanal Chem.*, 759 (2015) 137.
18. Q. T. Huang, X. F. Lin, C. Q. Lin, Y. Zhang, H.Q. Zhang, S. R. Hu, C. Wei and Q. X. Tong, *Anal. Methods*, 8 (2016) 6347.
19. Y. X. Zuo, J. K. Xu, K. X. Zhang, X. M. Duan, L. M. Lu, L. P. Wu, G. Ye, Y. S Zhang, H. K. Xing, L. Q Dong, H. Sun and X. F. Zhu, *Int. J. Electrochem. Sci.*, 11 (2016) 3776.
20. J. Tang and B. K. Jin, *J. Electroanal Chem.*, 780 (2016) 46.
21. R. Abdel-Hamid, F. Garcia, E. F. Newair and F. Garcia, *Br. J. Anal.Chem.*, 13 (2016) 38.
22. W. T. Lai, X. B. Li, W. C. Wang, X. Tian, X. Y. Wen, D. F. Fan, Z. Ma and W. Sun, *J. Hainan Normal Univ. (Natural Science)*, 28 (2015) 172.
23. M. Parthibavarman, V. Hariharan, C. Sekar, *Mater. Sci. Eng.*, C 31 (2011) 840.
24. P. Baraneedharan, S. Alexander, S. Ramaprabhu, *J. Appl. Electrochem.*, 46 (2016) 1.
25. N. Lavanya, E. Fazio, F. Neri, A. Bonavita, S.G. Leonardi, G. Neri and C. Sekar, *Sensor. Actuat. B-Chem.*, 221 (2015) 1412.
26. V. Srivastava and J. Jain, *Mater. Lett.*, 169 (2016) 28.
27. W. C. Wang, L. F. Dong, S. X. Gong, Y. Deng, J. H. Yu, H.Z. Dong, T. Y. Wang and W. Sun. *Arab. J. of Chem.*, <https://doi.org/10.1016/j.arabjc.2015.09.007>.
28. E. Laviron, *J. Electroanal. Chem.*, 101 (1979) 19.
29. J. Kang, X. Lu, H. Zeng, H. Liu and B. Lu, *Anal. Lett.*, 35 (2002) 677.
30. P. F. Pang, Y. P. Liu, Y. L. Zhang Y. T. Gao and Q. F. Hu, *Sensor. Actuat. B-Chem.*, 194 (2014) 397.
31. A. L. Liu, S. B. Zhang, L. Y. Huang, Y. Y. Cao, H. Yao and W. Chen, *Chem. Pharm. Bull.*, 56 (2008) 745.
32. S. H. Wu, S. H. Wu, B. J. Zhu, Z. X. Huang and J. J. Sun, *Electrochem. Commun.*, 28 (2013) 47.
33. A. C. Franzoi, I. C. Vieira, J. Dupont, C. W. Scheeren and L. F. de Oliveira, *Analyst*, 134 (2009) 2320.
34. G. J. Li, L. H. Liu, Y. Cheng, S. X. Gong, X. L. Wang, X. J. Geng and W. Sun, *Anal. Methods*, 6 (2014) 9354.
35. Z. R. Wen, X. Y. Li, X. L. Niu, W. S. Zhao, Y. Cheng, Q. W. Ma, X. B. Li, W. Sun and G. J. Li, *Int. J. Electrochem. Sci.*, 12 (2017) 4847.
36. D. B. Lu, S. X. Lin, L. T. Wang, T. Li, C. M. Wang and Y. Zhang, *J. Solid State Electr.*, 18 (2014) 269.
37. A. C. Franzoi, I. C. Dupont, C. W. Scheeren and L. F. de Oliveira, *Analyst*, 134 (2009) 2320
38. F. Gao, X. Chen, H. Tanaka, A. Nishitani and Q. Wang, *Adv. Powder Technol.*, 27 (2016) 921.

© 2017 The Authors. Published by ESG (www.electrochemsci.org). This article is an open access article distributed under the terms and conditions of the Creative Commons Attribution license (<http://creativecommons.org/licenses/by/4.0/>).